

## Lithofacies Delineation and Petrophysical Evaluation of Lower Miocene Reservoirs in the Rhoda Field, Onshore Niger Delta: An Application of Well-Log Data, Attribute Crossplotting and Petrophysical Analysis

Charles A. Illo\*, Mosto K. Onuoha, Kingsley Aghara

University of Nigeria, Nsukka, Department of Geology, Nigeria

Received February 25, 2021; Accepted July 2, 2021

---

### Abstract

Lithofacies classification and petrophysical properties evaluation plays an important role in reservoir description by reducing ambiguities connected to the increase in reservoir prediction. The lower Miocene reservoirs in the Rhoda field, onshore Niger Delta were affected by subsurface complexities mostly related to depositional and systematic effect of clay volume. In this study, well-log attribute crossplots were employed to correctly define lithofacies and petrophysical evaluation approaches to ascertain the reservoir properties of the sandstone intervals in OLU-121 well of the Rhoda field, Niger Delta. The crossplots of acoustic impedance with gamma-ray and velocity ratio were produced using the Hampson Russel software. The result of the crossplots populations shows four major lithofacies classified to be sandstone, sandy-shale, shaly-sand, and shale. Petrophysical analysis shows that two major lithofacies of sandstone and shale. D-3000, F-1000 and F-2000 reservoirs were found to be hydrocarbon saturated, while reservoir F-1500 was brine saturated. The average porosity of these reservoirs ranges between 0.180 to 0.320 frac. This study has shown that the crossplot technique can be utilized to better define reservoirs for further well development. It is worth mentioning that detailed characterization of subsurface reservoirs have important implications in the sustainability of reservoir performance.

**Keywords:** Lithofacies; Petrophysical properties; Acoustic impedance; Reservoir properties; Crossplot.

---

## 1. Introduction

Lithofacies description and petrophysical evaluation are indispensable features of reservoir characterization studies, due to key roles they play in predicting sustainability and producibility of reservoirs [1]. Effective classification of lithofacies with good understanding of certain geological factors like lithology, mineralogy, and diagenesis is essential for optimum hydrocarbon production through the application of reservoir models [2-3]. In achieving a reasonable reservoir depiction model, core samples and well-logs are commonly utilized due to the accuracy they have in vertical resolution [4]. However, due to the complexity of the Niger Delta basin, resulting from depositional and systematic effect of clay volume [5-6], these core and well-logs data show slight information about the distribution/classification of reservoir properties [1]. On the contrary, petrophysical parameters such as shale volume, water saturation and porosity, and rock physics attributes like acoustic impedance and velocity ratio generated from well-logs ensure better information on the distribution and quantitative reservoir characterization [7-10]. In this regard, good knowledge of lithofacies and petrophysical reservoir properties analysis could be achieved by integrating well-log attributes crossplots and petrophysical evaluation.

Over the past years, crossplotting of well-log attributes and petrophysical evaluation have contributed efficiently in hydrocarbon industries by reducing ambiguities connected to the characterization of reservoir properties, therefore refining reservoir assessments [9, 11-16]. Anyiam *et al.* [1] as well as Luo *et al.* [17] had established that lithologies such as sandstone, shale, and sand-shale intercalations, and certain reservoir properties like porosity and fluid

saturation, can be delineated using well-log crossplots (e.g. gamma-ray vs density, velocity-ratio vs porosity, velocity-ratio vs acoustic impedance). Senosy *et al.* [18] had also demonstrated that sand, shale and siltstone lithologies, with their associated fluid contents, and also certain reservoir parameters similar to porosity, water saturation and volume of shale, can be calculated through petrophysical evaluation.

The objective of this study is to provide a more detailed reservoir characterization on the identified reservoir units based on lithofacies and petrophysical properties through the application of crossplot populations [8] and petrophysical evaluations.

## 2. Geological setting

Rhoda field is located in the Coast Swamp Depobelt of the onshore Niger Delta basin (Fig. 1). The stratigraphic arrangement within the study area is formed from a major regressive cycle that resulted in the deposition of allocyclic units of transgressive marine sand, marine shale, shoreface and fluvial back swamp deposits [19-20].

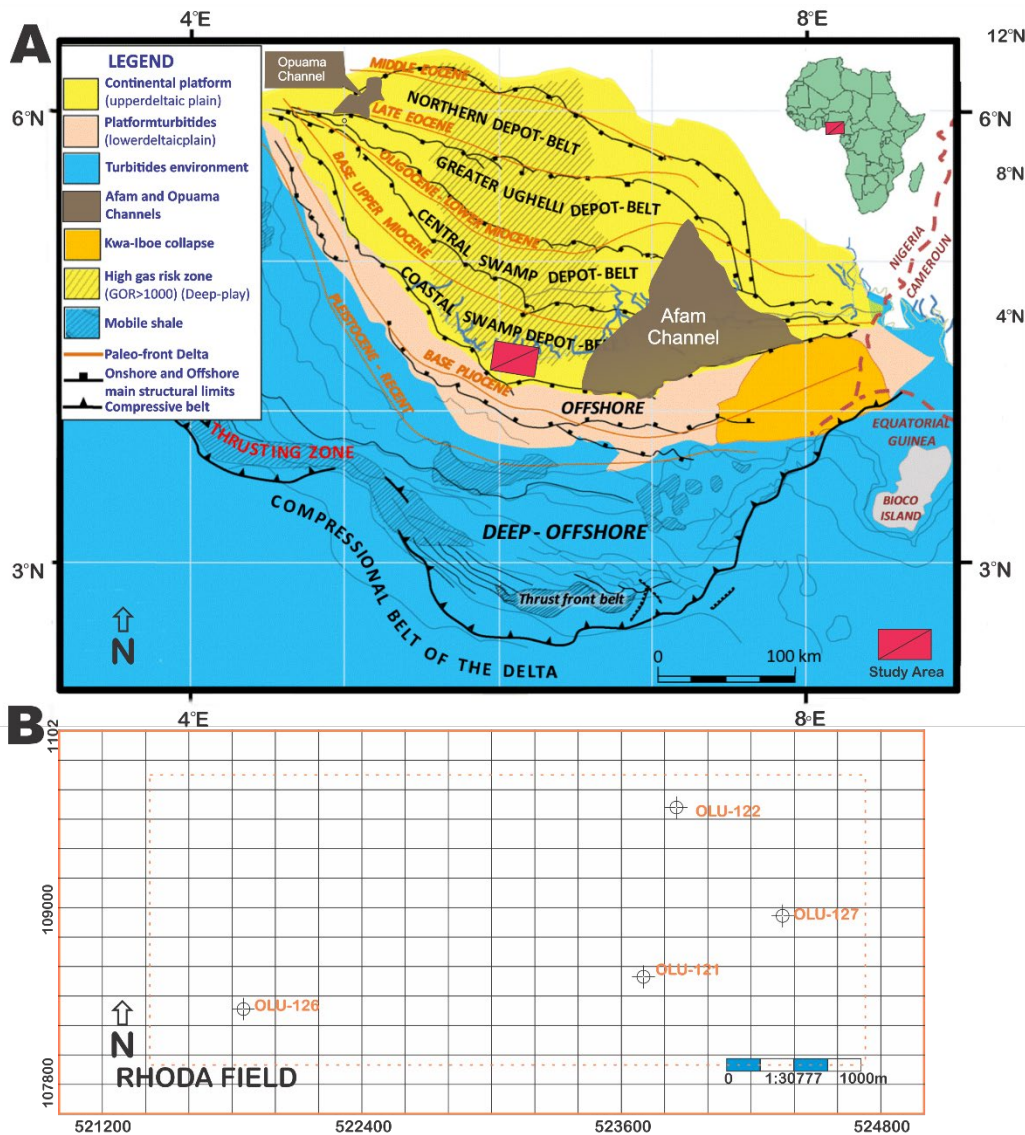


Fig. 1. Location map of studied area. (a) Map showing the location of Niger Delta Basin (modified after [20]). (b) Centralized focus on Niger Delta Basin displaying the studied Rhoda field and wellbore distribution across the survey

The three lithostratigraphic units in the study area starting from the top are the continental facies of Benin Formation, paralic delta front facies of Agbada Formation and pro-delta facies of Akata Formation (Fig. 2a). The Akata Formation which is the oldest of the three lithostratigraphic formations with age ranging from Eocene to recent, are characterized as deep marine shales representing the source rock [19, 21-22]. These marine shales are formed during the early development stages in Niger Delta progradation and are typically under-compacted and over-pressured. These shales also form diapiric structures including shale swells and ridges which often intrude into overlying Agbada Formation (Fig. 2b). The Agbada Formation is the major oil-producing formation in the Niger Delta Complex Basin, and overlies the Eocene Akata Formation, which is the principal source hydrocarbon source rock [23]. This Formation is estimated to be approximately 13,000 feet and bears the reservoir rock and seal for hydrocarbon build-up [24]. The upper part of the Agbada Formation is recent, the middle part comprises completely non-marine shale deposits, and the lower part, which extends to a depth of 4600 feet (ft), is defined by the earliest marine shale. The reservoir thickness within the Agbada Formation is seen within the range of limited feet smaller than 45ft (14 meters) to fewer feet above 150ft (46 meters), thinning toward down-thrown sides of growth faults [25]. The Benin Formation comprises the top part of the Niger Delta clastic wedge, from the Benin-Onitsha area in the north to beyond the coastline [21].

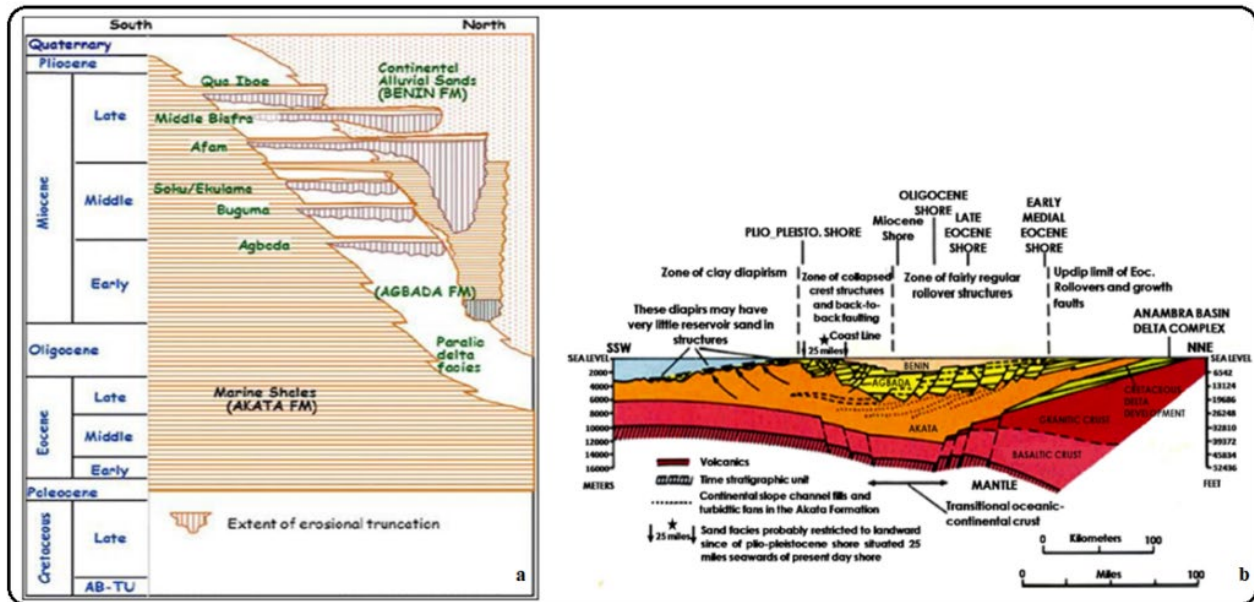


Fig. 2 a Stratigraphy of the Niger Delta showing the lithologic units of the three formations (adopted from [22]). b Generalized dip section of the Niger Delta showing the structural features of the Delta (adopted from [20])

The migration pathways of the Niger Delta basin stems from the existing structural features such as rolover anticlines, antithetic faults, collapsed crest faults, multiple growth faults, and back-to-back faults [19, 26-27], as seen in Fig. 2b with most of these faults offsetting at different parts of the Agbada Formation and flattening into Eocene detachment planes near the top of the Akata Formation [28].

### 3. Dataset and methods

#### 3.1. Dataset

The dataset used in the current study comprises the well log data which was provided by Shell Petroleum Development Company (SPDC), Nigeria. This data comprising well logs from

OLU-121well, obtained from the Rhoda Field of the Niger Delta, was analysed using the Hampson Russell software to display petrophysical and rock physics well log attributes, and related crossplots that were interpreted.

### 3.2. Methods

The well-log attributes such acoustic impedance (P-Impedance), and velocity ratio (VpVs\_Ratio) were first generated using the Hampson Russell software (Fig. 3) by applying the linear equations: P-Impedance =  $V_p \times \rho$  where  $V_p$  = p-wave in ft/s,  $\rho$  = density in g/cc;  $V_pV_s\_Ratio = V_p/V_s$  where  $V_s$  = s-wave in ft/s. After the successful generation of these attributes, crossplots of gamma-ray log with P-Impedance (Fig. 4a), and  $V_pV_s\_Ratio$  with P-Impedance (Fig. 5a) were generated using same Hampson Russell software. These crossplot populations were used to accurately delineate the different lithofacies and mark out the reservoir units for further petrophysical evaluations. Primary well logs such as gamma-ray, resistivity, density and sonic from OLU-121well were used for the evaluations. Then, the shale volume ( $V_{shale}$ ) was estimated (Fig 3, Track 4) using the [29] equation for Tertiary rocks;  $V_{shale} = 0.083(2(3.7 \times x) - 1)$ , where  $x$  represents the gamma-ray index. The interval of evaluation is 0.5 ft. Assessment of reservoir porosity was done (Fig 3, Track 8) using the density log (RHOB), which is given as  $\phi = \rho_{ma} - \rho_{obs} / \rho_{ma} - \rho_f$ , where  $\phi$  = porosity,  $\rho_{ma}$  = matrix density (sandstone = 2.65 grams/cc),  $\rho_{obs}$  = log density,  $\rho_f$  = fluid density (fresh water = 1.09 grams/cc). Water saturation ( $S_w$ ) was evaluated (Fig 3, Track 6) using [11] equation;  $S_w^n = a/\phi^m \times R_w / R_t$ , where  $a$  = cementation factor (1),  $m$  = cementation exponent (1.8),  $n$  = saturation exponent (1.9),  $R_w$  = resistivity formation water (0.65),  $R_t$  = true formation resistivity.

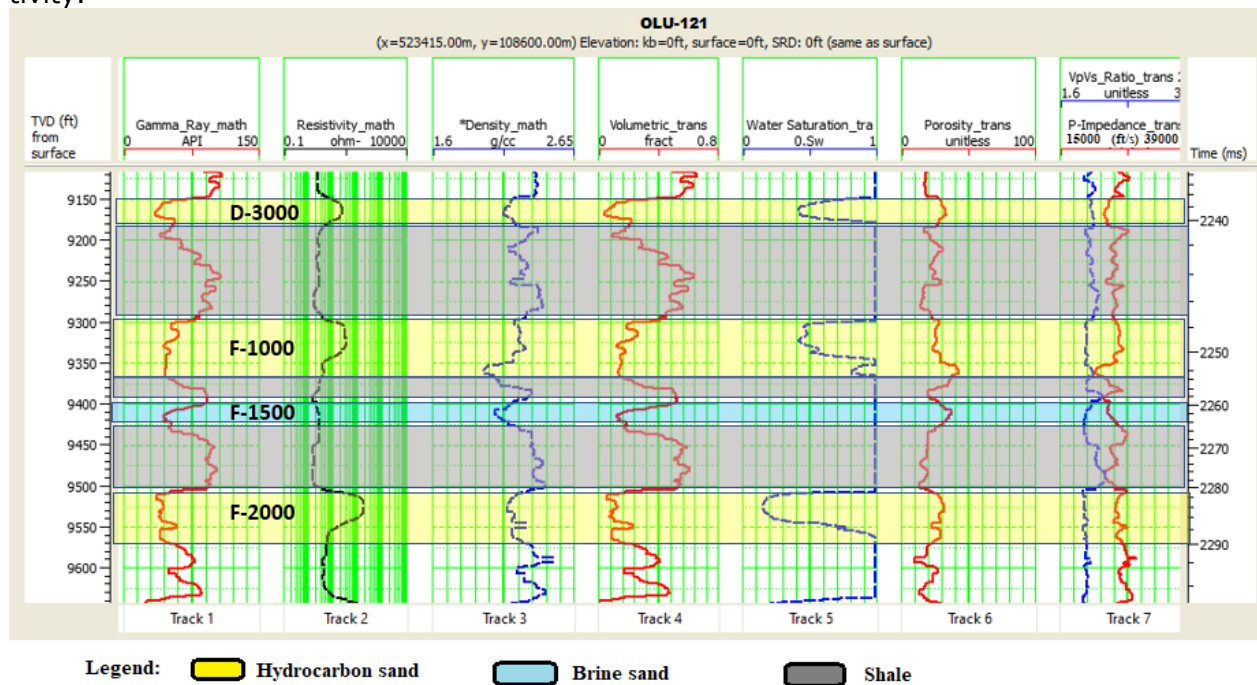


Fig. 3. Well logs display showing lithologic relationship across logs in OLU\_121 well. Observe sandstone lithology at the upper section of both reservoirs with low gamma ray and high resistivity value

## 4. Result description and interpretation

### 4. 1. Lithofacies characterization using well-log attribute crossplot models

#### 4.1.1. Description

Fig. 4(a, b) reveals well attribute crossplot and cross-section respectively of gamma-ray vs P-Impedance generated from OLU-121well. Four populations represented with colours such

as yellow, red, aqua blue and blue characterizes different lithologies (Fig. 4a). The colour scheme and colour attribute used in the interpretation of these populations were lithology and Vshale (volumetric) respectively. The Vshale display values that ranges between 0.00 – 0.72 fraction. These values increase with increasing amount of shale which were clearly represented in the crossplot domain (Fig. 4a). The gamma-ray and P-Impedance values range from 40 – 105 API and 21000 – 28000 (ft/s) \* (g/cc) respectively. These well attributes increase with more presence of shale and decreases towards sand compartments (Fig. 4a).

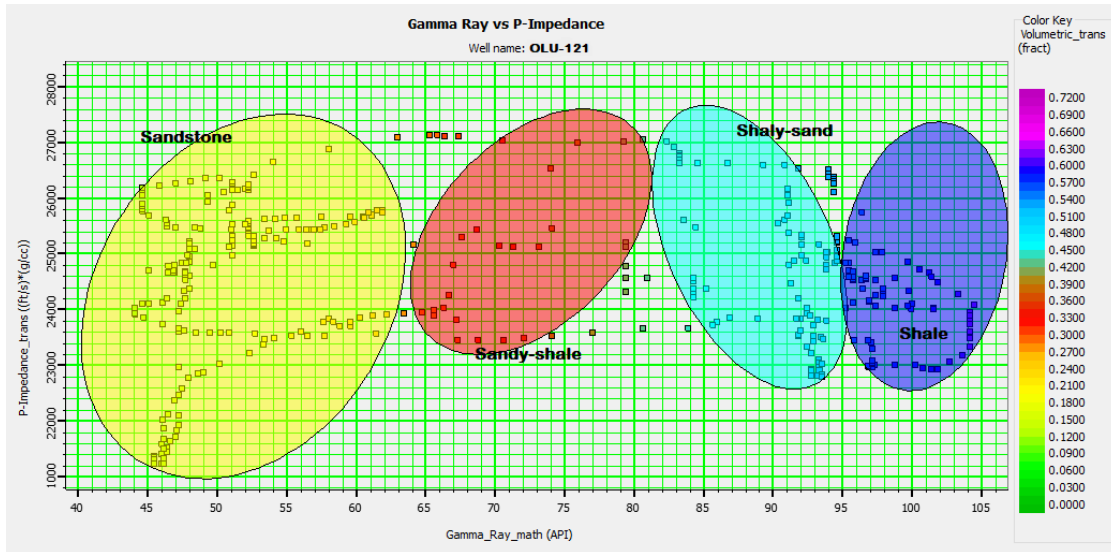


Fig. 4a. Gamma-ray versus acoustic impedance (P-Impedance) crossplot for F-1000 and F-2000 reservoirs in OLU-121 well

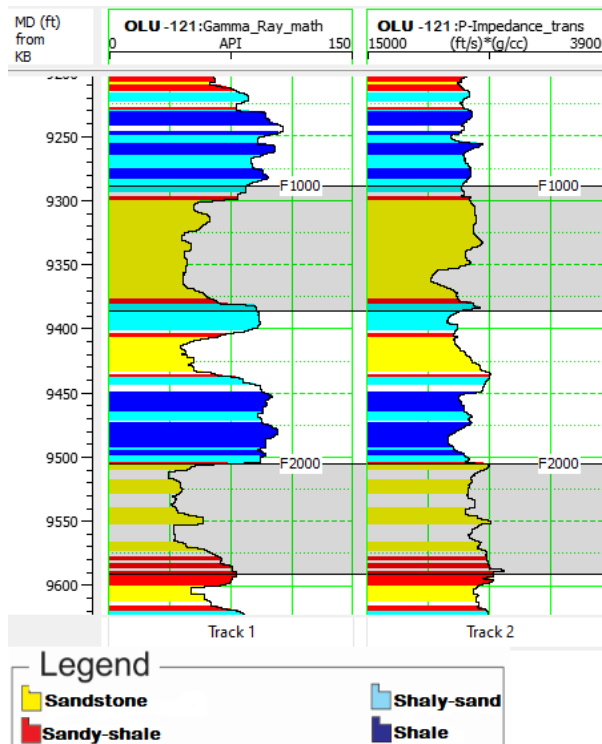


Fig. 4b. Well attribute cross-section of gamma-ray and acoustic impedance (P-Impedance) for F-1000 and F-2000 reservoirs. Observe the discrimination of various lithologies within the examined reservoirs with colour codes

Fig. 5(a, b) reveals also the well attribute crossplot and attribute cross-section of VpVs\_Ratio and P-Impedance from the examined OLU-121 well. Four populations signified with green, yellow, red and black colours were used to delineate the reservoir lithology (Fig. 5a). Lithology and water saturation were selected as the colour scheme and colour attribute respectively for the understanding of various populations. Water saturation show values that ranges from 0.01 – 1.00 (0.Sw). These values that increases with the increasing amount of brine in rocks were used to delineate populations represented in the crossplot domain (Fig. 5a). The VpVs and P-Impedance attribute values fall between 1.85 – 2.15 and 21000 – 27500 (ft/s) \* (g/cc) respectively. The VpVs attribute is more sensitive to fluids and was used in lithological classification given that, sandstone lithology represents more of a possible hydrocarbon accumulator due to its high porosity features, while shale represents more of brine saturation as a result of its high cementation effects and low porosity.

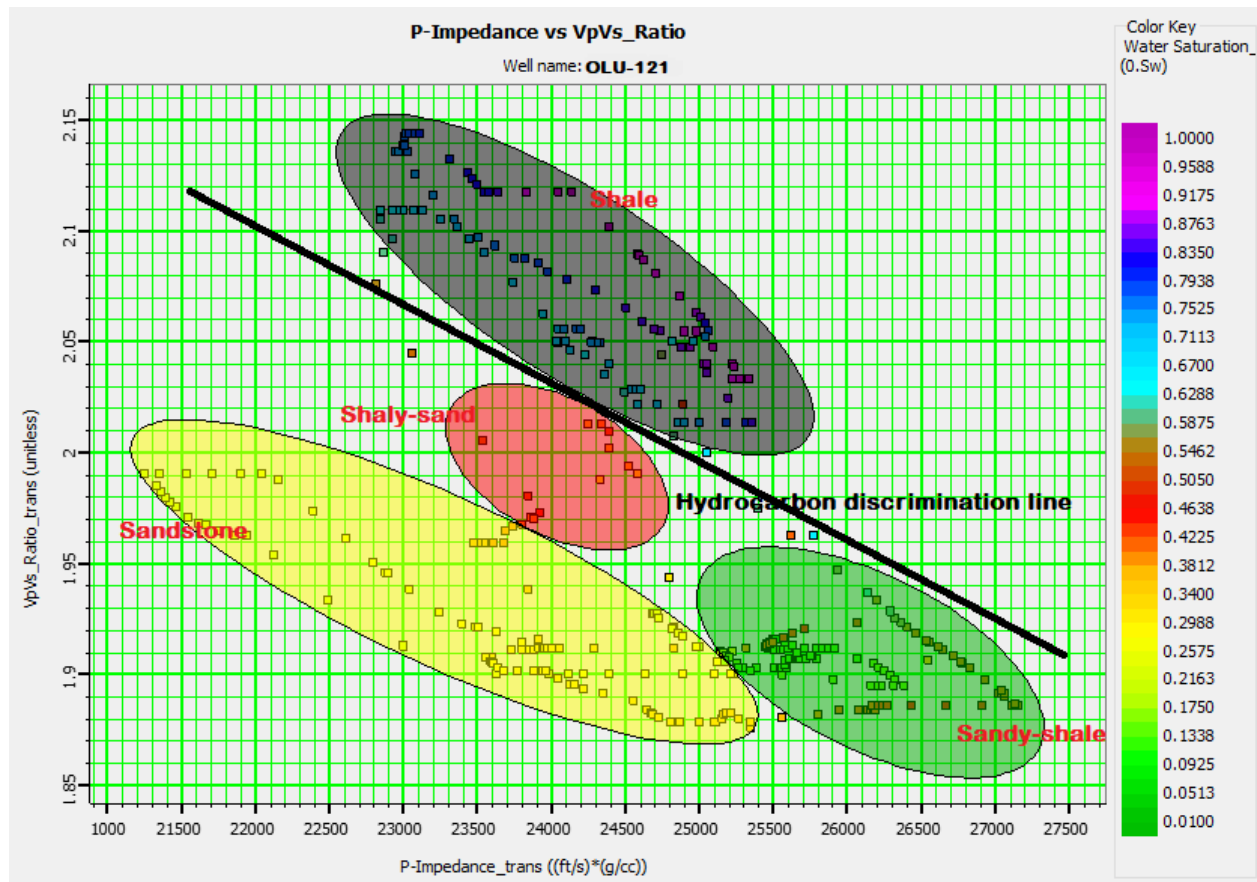


Fig. 5a. VpVs\_Ratio versus acoustic impedance (P-Impedance) crossplot for F-1000 and F-2000 reservoirs in OLU-121 well

Fig. 4b and 5b shows the attribute cross-sections generated from crossplot domains in Fig. 4a and 5a respectively. These cross-sections discriminate reservoirs from non-reservoirs, and also shows the sensitivity of these well log attributes to reservoir sandstone formation. The legends represented below (Fig. 4b, 5b), were used in identifying various lithologies using colour codes.

**4.1.2. Interpretation**

The yellow population associated with low values of Gamma-Ray ranging between 0 – 62 API, and moderate to low values of P-Impedance ranging from 21,200 – 26,800 (ft/s) \* (g/cc) (Fig. 4a) were interpreted as sandstone lithology. The observed lower values of the Gamma-Ray suggest possible effect of high net-to-gross ratio [9]. The red population linked with mod-

erate to low values of Gamma-Ray ranging from 64 – 79 API, and moderately-low P-Impedance values that falls between 23,200 – 27,000 (ft/s) \* (g/cc) (Fig. 4a), correspond to sandy-shale lithology [20]. These observed moderately-low values of Gamma-Ray represented with red population could be related to little increase of shale intercalation to sand [9]. The light-blue population associated with moderate to high values of Gamma-Ray ranging between 82 – 94 API, and moderate values of P-Impedance ranging from 22,800 – 27,000 (ft/s) \* (g/cc) (Fig. 4a) were interpreted as shaly-sand lithology [20]. The moderately-high gamma-ray values suggest large increase of shale intercalation to sand (large decrease in net-to-gross ratio), compared to the red population characterized to be sandy-shale [9]. The blue population related to high values of gamma-ray ranging between 82 – 94 API, and moderate P-Impedance values ranging from 24,200 - 32800 (ft/s) \* (g/cc) (Fig. 4a), correspond to shale lithology [20]. The observed high gamma-ray values indicate low-rigidity modulus and high densities associated with shale. The well attribute cross-section (Fig. 4b) discriminates reservoirs F-1000 and F-2000 from non-reservoir zones. The dominant yellow colouration associated with F-1000 and F-2000 reservoirs in the well cross-section (Fig. 4b), correspond to sandstone lithology, while low display of red and light-blue colours represented in little proportion towards the top and base of F-1000 reservoir (Fig. 4b), corresponds to sandy-shale and shaly-sand lithologies respectively [1, 8].

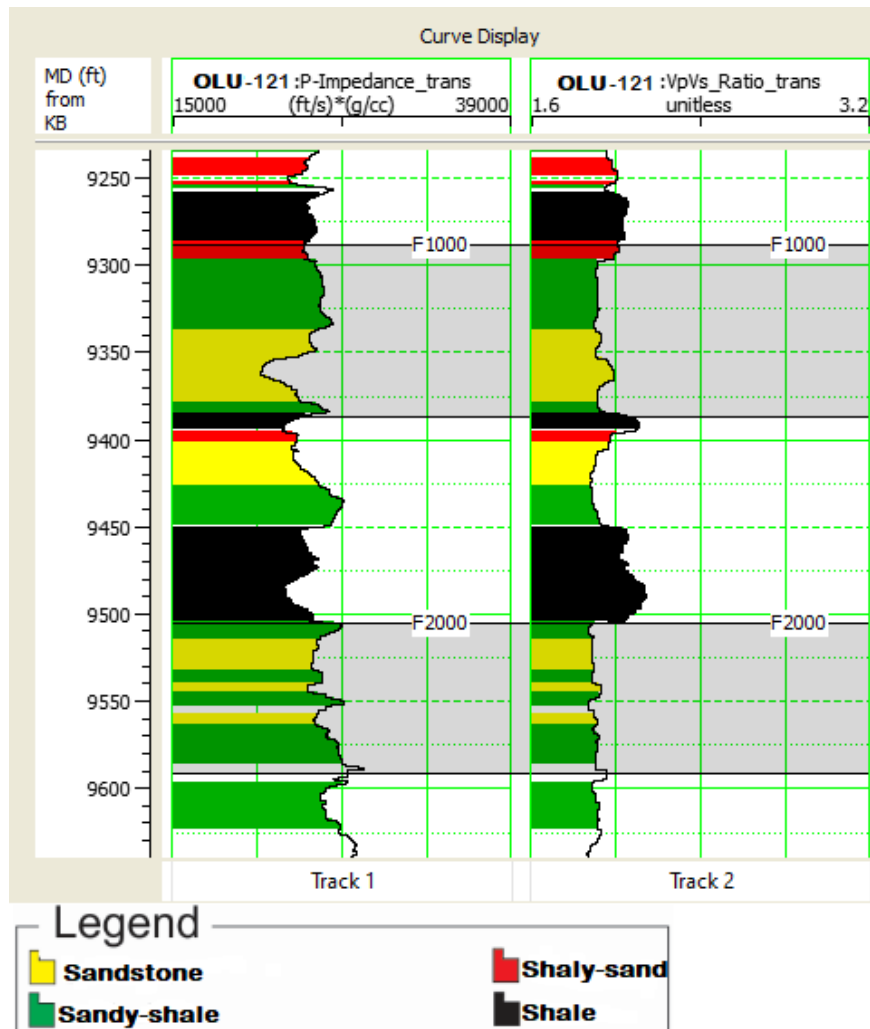


Fig. 5b. Well attribute cross-section of VpVs\_Ratio and acoustic impedance (P-Impedance) for F-1000 and F-2000 reservoirs. Observe also lithologic differentiation within the examined reservoirs with colour codes

The yellow population connected with low values of VpVs\_Ratio ranging between 1.87 – 1.99, and moderately low P-Impedance values that falls below 25,400 (ft/s) \* (g/cc) (Fig. 5a) were interpreted as sandstone lithology [8]. The noticed lower values of the VpVs\_Ratio could be seen from effects of high-incompressibility and lighter fluid (hydrocarbon) saturation [9]. The green population associated with low values of VpVs\_Ratio ranging from 1.88 – 1.95, and moderate to high P-Impedance values that falls between 25,200 – 27,200 (ft/s) \* (g/cc) (Fig. 5a), correspond to sandy-shale lithology. The observed moderate to high P-Impedance values suggests low to moderately-high compressibility of sandy-shale due to slight increase in shale. The red population connected with moderate values of VpVs\_Ratio and P-Impedance that ranges between 1.97 – 2.01 and 23,500 – 24,600 (ft/s) \* (g/cc) respectively (Fig. 5a) were interpreted as shaly-sand lithology). The observed average values of these attributes suggest moderate to high compressibility of the rock due to increasing amount of shale and likely presence of denser fluid (brine). The black population associated with moderate to high values of VpVs\_Ratio ranging from 2.01 – 2.15, and moderate P-Impedance values that fall between 22,800 – 25,400 (ft/s) \* (g/cc) (Fig. 5a), correspond to shale lithology. The observed moderate to high values of VpVs\_Ratio for shale, compared to sand suggests low-rigidity modulus and high presence of brine saturation (see also [9-10]). The yellow and green colours connected with F-1000 and F-2000 reservoirs in the well cross-section (Fig. 5b) were correspondingly interpreted as sandstone and sandy-shale lithologies, while the red colour towards the upper part of F-1000 reservoir, corresponds to shaly-sand lithology [8]. The diagonal black thick line associated with the crossplot domain (Fig. 5a) was interpreted as the hydrocarbon discrimination line. The observed black line suggests potential hydrocarbon zones to be yellow, green and red populations, and brine saturation compartment to be the black population [20].

**4.1.3. Description**

As seen from the gamma-ray log (Fig. 3, Track 1), four distinctive reservoirs described as D-3000, F-1000, F-1500 and F-2000 were delineated. The three reservoirs represented with yellow colours display a blocky depositional style, except the tiny blue colour F-1500 reservoir that shows a coarsening upwards depositional trend. High resistivity and moderate to low density responses correspond to low gamma-ray values for reservoirs represented with yellow colour, while low resistivity and moderately-low density values correspond to low gamma-ray response for blue coloured F-1500 reservoir. Other well intervals represented with grey colour displays low resistivity and moderate to high density values that corresponds to high gamma-ray responses. Petrophysical properties such as Vshale, water saturation and porosity display low values within reservoirs interval which corresponds to high resistivity and low gamma-ray responses. Rock physics attributes like P-impedance and VpVs\_Ratio displayed in track 7 of the well section (Fig. 3) showed low values of VpVs\_Ratio, and moderate to low values of P-Impedance within the reservoir intervals, which corresponds to high resistivity and low-gamma-ray responses. Estimated Vshale and porosity for the reservoirs display low values ranging between 0.334 and 0.452 frac, and 0.180 – 0.320 frac respectively (Table 1). The water saturation reveals low values ranging between 0.356 – 0.450 for the yellow-coloured reservoirs, and a high value of approximately 0.945 frac for the blue coloured F-1500 reservoir (Table 1).

Table 1. Summary of petrophysical results from OLU-121well

Reservoir units	Interval (ft)	Net Sand (Ft)	Average porosity (Frac)	Average water saturation (Frac)	Average V-shale (Frac)
D-3000	9150 - 9176	0.625	0.320	0.415	0.375
F-1000	9289 - 9386	0.691	0.280	0.450	0.334
F-1500	9400 - 9425	0.585	0.260	0.945	0.452
F-2000	9505 - 9592	0.678	0.180	0.358	0.440

#### 4.1.4. Interpretation

The reservoir intervals delineated with yellow colour, associated with high resistivity and moderate to low density values that correspond to low gamma-ray values (Fig. 3) were interpreted as hydrocarbon-saturated sandstone lithology [20]. The tiny reservoir interval described with blue colour, associated with low resistivity, moderately-low density and high-water saturation values corresponding to low gamma-ray response (Fig. 3) was interpreted as brine-saturated sandstone. The intervals displayed in grey colour which is connected with low resistivity and moderate to high density values that relates to high gamma-ray responses (Fig. 3), correspond to shale lithology. The low Vshale values associated with the reservoirs (Fig. 3) correspond to clean sandstone units [1]. The low porosity values associated with the reservoirs (Fig. 3, Table 1) suggest good porosity features capable of maintaining a steady fluid flow [1]. The low water saturation values connected with D-3000, F-1000 and F-2000 reservoirs (Fig. 3, Table 1), correspond to sandstone reservoirs saturated with more hydrocarbon fluid, compared to brine fluid. This interpretation was supported with high resistivity and low-density response within the reservoir intervals. The high values of water saturation associated with F-1500 reservoir (Fig. 3, Track 1) was interpreted as brine saturated sandstone reservoir. This interpretation was confirmed with the low gamma-ray and low resistivity response of the reservoir unit.

### 5. Discussion

Based on the analysis results from direct and indirect equations on OLU-121 well-log data of the Rhoda field, the crossplotting analysis and petrophysical evaluations as an appropriate method were used for thorough reservoir characterization in prediction of lithofacies and petrophysical properties of the reservoir sandstone units. The results from crossplot analysis show that significant part of the reservoir sandstones in the Rhoda field are characterized by low values of gamma-ray and VpVs\_Ratio that corresponds to low values of Vshale and water saturation, as they are considered as porous hydrocarbon sandstones. Wide variations in gamma-ray and VpVs\_Ratio from low to high values that are related to depositional and systematic effect of clay volume of sandstones in the field, can be considered as an indication showing variations in net-to-gross, and fluid content of the reservoir sandstones. In other words, low gamma-ray and VpVs\_Ratio are compatible with clean sandstones and hydrocarbon fluid saturation and vice versa. These means that sandstones lithofacies with low gamma-ray values are cleaner than those with moderately-high values for this parameter. Also, lithofacies with low values of VpVs\_Ratio are more likely to be hydrocarbon sands than those with moderate and high values. So, gamma-ray and VpVs\_Ratio can be used as main well-log attributes in the characterization of lower Miocene reservoirs in the Rhoda field. The well-logs section of predicted petrophysical properties from OLU-121 well are shown in Fig. 3 (Track 4, 5 and 6). The results from the three petrophysical properties estimated to be Vshale, water saturation and porosity indicate that low values of these properties correspond to high resistivity and low gamma-ray responses which are directly associated with hydrocarbon reservoir sandstones in the Rhoda field. This means more porous sandstones with high resistivity are basically more clean sand with hydrocarbon fluid. Based on these results, the well intervals are classified into 3 main zones based on the variations of these well-log attributes which are in accordance to depositional and clay volume effects of the lithological units.

The reservoir delineation results using well-log attribute crossplots from OLU-121 well reveals distinct lithofacies of sandstone, sandy-shale, shaly-sand and shale, which agrees with results of [1] in their application of crossplots in lithology delineation and petrophysical evaluation of three wells in the western Coastal Swamp, Niger Delta, and [20] in their application of crossplots and prestack seismic-based impedance inversion for discrimination of lithofacies and fluid prediction in an old producing field, Eastern Niger Delta Basin.. However, the crossplotting models and petrophysical evaluations make an understanding of the distribution and quality of the lower Miocene reservoirs of the Niger Delta basin in the studied field. The results

obtained in this study can be used as a powerful tool for risk reduction in achieving a more quantitative characterization of these reservoir sandstones to maximize production.

## 6. Conclusion

This present study reveals the utilization of well-log data, crossplot techniques and petrophysical evaluations in the investigation of lithofacies and petrophysical properties of lower Miocene reservoirs in the Rhoda field, onshore Niger Delta. To reach this goal, well-log data were evaluated, followed by the application of direct and indirect relationships (log transforms) to produce certain petrophysical parameters like porosity, water saturation and shale volume, and rock physics properties such as acoustic impedance and velocity ratio. The crossplot of Gamma-ray and P-Impedance, with Vp/Vs\_Ratio and P-Impedance shows that the examined reservoirs are classified into four lithological groups, which are sandstone, sandy-shale, shaly-sand, and shale. The results also confirmed the probable zones of hydrocarbon accumulation (left-hand side) through the delineation of hydrocarbon discrimination line. The petrophysical results confirmed that the reservoirs are moderately clean, containing clay volumes showing low values of 0.375, 0.334, 0.452 and 0.440 frac for D-3000, F-1000, F-1500 and F-2000 reservoirs respectively. The water saturation reveals moderate to low values of 0.415, 0.450 and 0.358 frac for D-3000, F-1000 and F-2000 respectively which are classified to be hydrocarbon reservoir sandstones, and high value of about 0.945 frac for F-1500 reservoir categorized to be brine saturated sand. Similarly, the porosities of the reservoir units are good, indicating low porosity values across the reservoirs to be 0.320, 0.280, 0.260 and 0.180 frac for D-3000, F-1000, F-1500 and F-2000 respectively. These low porosity values encourage free fluid-flow within the pore spaces of rock. Conclusively, the generated crossplotting models and petrophysical evaluations can stand as a premise for quantitative seismic interpretation, thus reducing risks connected to prospect evaluation.

## Acknowledgment

The authors are grateful to Shell Petroleum Development Company (SPDC), Port Harcourt, Nigeria, for providing the dataset used for this study for a Doctoral Research Program and also to the Geology Department, University of Nigeria, Nsukka, Nigeria, for their relentless assistance in providing a favourable workstation for this research.

## Funding

No funding was received for this research.

## Conflict of interest

The authors declare that they have no competing interests.

## Availability of data and material

Data was provided by permission.

## Authors' contributions

**Charles Afamefuna Illo:** Conceptualization, Methodology, Software, Formal analysis, Writing – original draft, Project administration. **Mosto Kalu Onuoha:** Supervision, Writing – review & editing, Validation. **Kingsley Aghara:** Software, Validation, Formal analysis.

## References

- [1] Anyiam OA, Mode AW, Okara ES. The use of cross-plots in lithology delineation and petrophysical evaluation of some wells in the western Coastal Swamp, Niger Delta. *J. Pet. Explor. Prod. Technology*. 2018; 8: 61-71.
- [2] Jennette D, Wawrzyniec T, Fouad K, Dunlap DB, Meneses-Rocha J, Grimaldo F, Munoz R, Barrera D, Williams-Rojas CT, Escamilla-Herrera A. Traps and turbidite reservoir characteristics from a complex and evolving tectonic setting, Veracruz Basin, Southeastern Mexico. *AAPG Bulletin*. 2003; 10(10):1599–1622.

- [3] Feng R, Luthi SM, Gisolf D, Angerer E. Reservoir lithology classification based on seismic inversion results by Hidden Markov Models: Application prior geological information. *Mar. Pet. Geol.* 2018; 93:218–229.
- [4] Soto R, Holditch SA. Development of reservoir characterization models using core, well log, and 3D seismic data and intelligent software. *Soc. Pet. Eng. Inc.* 2010; 57457:1–13
- [5] Asquith N. Basic well log analysis for geologists, *Methods in exploration.* Am. Assoc. Pet. Geol. 2004; 16:12 – 135
- [6] Prakoso S, Burhannudinnur M, Yasmaniar G, Rahmawan S, Irham S. A systematic effect of clay volume on porosity – p-wave velocity relationship. *J. Phy. Confr. Series.* 2019; 1402:1-8.
- [7] Chopra S, Alexeev V, Xu V. 3D AVO Crossplotting – an effective visualization technique, SEG technical program expanded abstracts. 2003; 189-192
- [8] Odegaard E, Avseth P. Well log and seismic data analysis using rock physics templates, *First Break.* 2004 2337-43.
- [9] Avseth P, *Explorational rock physics: the link between geological processes and geophysical observables.* Bjørlykke K., Ed.; Springer-Verlag. Berlin Heidelberg, 2010; pp. 403-426,
- [10]. Avseth P, Veggeland T. Seismic screening of rock stiffness and fluid softening using rock-physics attributes, *Interpretation.* 2015; 3(4):85-93,
- [11] Archie GE. The electrical resistivity log as an aid in determining some formation characteristics. *Trans. Am. Inst. Min. Metall. Eng.* 1942; 146:54-62
- [12] Hilchie DW. *Applied openhole log interpretation,* DW Hilchie, Inc, Golden, Colorado. 1978; p.161
- [13] Szabó NP. Shale volume estimation based on the factor analysis of well-logging data. *Acta Geophys.* 2011; 59(5):935-953..
- [14] Chatterjee R, Paul S. Application of cross-plotting techniques for delineation of coal and non-coal litho-units from well logs in Jharia Coalfield, India, *Geomaterials.* 2012; 2:94-104
- [15] Das B, Chatterjee R. Well log data analysis for lithology and fluid identification in Krishna-Godavari Basin, India, *Arab. Jour. Geosci.* 2018; 11, 231,
- [16] Abbey CP, Okpogo EU, Atueyi IO. Application of rock physics parameters for lithology and fluid prediction of TN field of Niger Delta Basin, Nigeria. *Egy. J. Pet.* 2018; 27(4):853-866.
- [17] Luo Y, Huang H, Jakobsen M, Yang Y, Zhang J, Cai Y. Prediction of porosity and gas saturation for deep-buried sandstone reservoirs from seismic data using an improved rock-physics model, *Acta. Geophys.* 2019; 67:557-575,
- [18] Senosy AH, Ewida HF, Soliman HA, Ebraheem MO. Petrophysical analysis of well logs data for identification and characterization of the main reservoir of AI Baraka oil field, Komombo Basin, Upper Egypt, *SN App. Sci.* 2020; 2, 1293.
- [19] Reijers TJA. Stratigraphy and sedimentology of the Niger-Delta, *Geologos.* 2011; 17(3):133-162.
- [20] Okeugo CG, Mosto KM, Ekwe CA, Anyiam OA, Dim DP. Application of crossplot and prestack seismic-based impedance inversion for discrimination of lithofacies and fluid prediction in an old producing field, Eastern Niger Delta Basin. *J.Pet. Explor. Prod. Tech.* 2018; 9:97-110
- [21] Short KC, Stauble AJ. Outline of geology of Niger Delta. *Am Asso. Pet. Geol. Bull.* 1967; 51:761–779
- [22] Lawrence SR, Monday S, Bray R. Regional geology and geophysics of the eastern Gulf of Guinea (Niger Delta to Rio Muni), *Lead Edge.* 2002; 21:1112–1117
- [23] Chukwu GA. The Niger Delta complex basin: stratigraphy, structure and hydrocarbon potential, *J. Pet. Geol.* 1991; 14:211-220.
- [24] Doust H, Omatsola E. Niger Delta *Am. Assoc. Pet. Geol. Bull.* 1989:48 201–238.
- [25] Weber KJ, Daukoru E. Petroleum geology of the Niger Delta, *Proceedings of the Ninth World Petroleum Congress.* 1975; 2:209–221.
- [26] Evamy BD, Haremboure J, Kamerling P, Knaap WA, Molloy FA, Rowlands PH. Hydrocarbon habitat of tertiary Niger Delta. *Am. Asso. Pet. Geol. Bull.* 1978; 62:277-298
- [27] Stacher P. Present understanding of the Niger Delta hydrocarbon habitat, *Geology of deltas.* Oti, MN, Postma G, Eds., Balkema, Rotterdam, pp 257–268.
- [28] Reijers JTA, Petters SW, Nwajide CS. The Niger Delta Basin, African basins. *Sedimentary Basins of the World.* Selley RC, Ed., Elsevier, Amsterdam. 1997; 3:145–168
- [29] Larionov WW. Borehole radiometry, Nedra, Moscow. 1969; p.127
- [30] Ebong ED, Akpan AE, Urang JG. 3D structural modelling and fluid identification in parts of Niger Delta Basin, southern Nigeria. *J. Afri. Earth Sci.* 2019; 158:103565.

To whom correspondence should be addressed: Charles A. Illo University of Nigeria, Nsukka, Department of Geology, Nigeria, E-mail: [illocharles7@gmail.com](mailto:illocharles7@gmail.com)